

# P2X7 receptor large pore signaling in avian Müller glial cells

Robson X. Faria<sup>1</sup>  · Hercules R. Freitas<sup>2</sup> · Ricardo A. M. Reis<sup>2</sup>

Received: 5 December 2016 / Accepted: 11 May 2017 / Published online: 1 June 2017  
© Springer Science+Business Media New York 2017

**Abstract** ATP is a pleiotropic molecule that promotes extra- and intracellular signaling to regulate numerous functions. This nucleotide activates purine and pyrimidine receptors at the plasma membrane, categorized as ionotropic P2X or G-protein-coupled receptor (GPCR) P2Y receptors. P2X are ligand-gated ion channel receptors, expressed in both retinal neurons and Müller cells leading to neuron-glia communication, calcium waves and neurovascular coupling. However, how P2X pore is formed upon ATP activation and how signaling pathways regulates the complex is still a matter of controversy. Here we studied the properties of the P2X7 receptor (P2X7R) using electrophysiology, single cell Ca<sup>2+</sup> imaging, and dye uptake assay in purified avian Müller glia in culture. Our data show that ATP (or benzoyl-benzoyl ATP, BzATP) evoked large inward currents in patch-clamp studies while addition of P2X7R antagonist such as brilliant Blue G (BBG), abolished these currents. Ruthenium red (RU-2), a general

transient receptor potential (TRP) inhibitor, reduced currents induced by ATP. Our data also point to the involvement of mitogen activated protein kinase (MAPK), phosphoinositide 3-kinase (PI3K), Ca<sup>2+</sup>-calmodulin kinase II (CAMKII), microtubules or protein kinase C (PKC) modulating ATP-induced ionic current in Müller cells. We show that ATP induced Ca<sup>2+</sup> influx, partially inhibited by P2X7R antagonists (oxidized ATP or BBG), and totally inhibited by blockers of other pores such as transient receptor potential (TRPs) or connexin hemichannel. Additionally, MAPK, PKC, PI3K or CAMKII inhibitors also are involved in the modulation of intracellular calcium signaling. Finally, ATP induced 80–90% of dye uptake in Müller glia cells, while oxidized ATP (oATP), BBG or A740003 inhibited this effect. We conclude that large conductance channel and other P2XRs are not involved in the ATP-induced dye uptake, but signaling pathways such as MAPK, PI3-K, microtubules or PKC are involved in pore formation.

**Electronic supplementary material** The online version of this article (doi:10.1007/s10863-017-9717-9) contains supplementary material, which is available to authorized users.

✉ Robson X. Faria  
robson.xavier@gmail.com

Hercules R. Freitas  
freitashr@biof.ufjf.br

Ricardo A. M. Reis  
ramreis@biof.ufjf.br

<sup>1</sup> Laboratory of Toxoplasmosis and other Protozoans, Oswaldo Cruz Institute, Oswaldo Cruz Foundation (FIOCRUZ), Rio de Janeiro, Brazil

<sup>2</sup> Laboratory of Neurochemistry, Institute of Biophysics Carlos Chagas Filho, Universidade Federal do Rio de Janeiro, Cidade Universitária, Ilha do Fundão, Rio de Janeiro, RJ 21941-902, Brazil

**Keywords** P2X7 receptor · Pore formation · Dye uptake · Avian · Müller glial cells · Intracellular signaling

## Introduction

ATP has been recognized as a neurotransmitter since the 1970's (Burnstock 2015) and as a gliotransmitter in last two decades (Butt 2011; Verderio and Matteoli 2011). Cloning and identification of receptors for purine and pyrimidine occurred in the 1990's, with identification of several P2X ligand-gated ion channels receptor subtypes (Bartlett et al. 2014). ATP also activates numerous receptor subtypes of the GPCR P2Y subfamily (Jacobson and Muller 2016).

ATP induces the formation of ion channels in diverse cell types including glial cells (Magni and Ceruti 2014) such as astrocytes (Newman 2015), microglia (Skaper 2011) and

Schwann cells (Verkhatsky and Steinhauser 2000). Among P2 receptors, P2X7R has been involved in the regulation of considerable functions in the CNS, particularly in neuron-glia communication (Tewari and Seth 2015) and retinal degeneration and regeneration (Reichenbach and Bringmann 2016). This receptor is known to participate in the modulation of GABA and glutamate release (Barros-Barbosa et al. 2015) as well as pro-inflammatory cytokines release (Volonte et al. 2012) in glia or in neurons. Essentially, its pro-inflammatory functions are exacerbated in the eye, mediating diverse inflammatory events (Tong et al. 2016), and Müller cells possess a critical role in this process (Eastlake et al. 2016).

Müller glial cells are activated by glutamate through NMDA and non-NMDA receptors and these cells release ATP through a calcium-dependent exocytotic mechanism (Loiola and Ventura 2011). The same group also evaluated the role of ATP on survival of avian embryonic retinal cells in culture. They observed that ATP or BzATP (a P2X7R agonist) evoked apoptosis of developing retinal neurons in an early period of retinal development. This effect was glutamate-independent (but P2X7R-dependent) and it only happened when these cells were co-cultured with glial cells. Additionally, they exhibited a P2X7R dependent inhibition of [<sup>3</sup>H]-D-aspartate uptake and ethidium bromide uptake after agonist treatment (Ancasí et al. 2013). Recently, we evaluated the role of the antioxidant glutathione (GSH) in retinal neurons and glia cells (Freitas et al. 2016). GSH induced calcium shifts in Müller glial cells, but not in neurons. We also reported that GABA was released upon GSH stimulus in chick embryonic retina, mixed neuron-glia or Müller cell cultures. These effects were mediated by P2X7R, since BBG inhibited GSH-induced GABA release. Similarly, GSH induced dye uptake in Müller glial cell in a P2X7R dependent manner. Although these results are sufficient to demonstrate the participation of P2X7R in avian Müller cells, it is still an open matter how ATP mediates P2X7R ionic channel and pore formation, and its signaling. P2X7R is a trimeric channel with three binding sites for ATP (Yan et al. 2010), and it is unknown how the opening states lead to small or large pores. The transition of P2X7R activation and the large pore dynamics seems to involve at least two steps and might be regulated by several signaling pathways in different cells (Faria et al. 2016, 2010, 2009, 2005). Here, we used electrophysiology, calcium imaging and dye uptake assays to allow a functional read-out of avian Müller glia P2X7 response and how these different approaches are related to intracellular signaling pathways, using selective inhibitors.

## Methods

Fertilized white Leghorn eggs were purchased from a local hatchery. The embryos were staged according to

(Hamburger and Hamilton 1951) and sacrificed by decapitation on embryonic day 9 (E9). The eyes were removed and the retinas were dissected out in a Ca<sup>2+</sup>- and Mg<sup>2+</sup>-free Hanks' (CMF) solution. The retinas were then used to prepare cultured Müller glia cells essentially as recently described before (Freitas et al. 2016; Schitine et al. 2015).

## Chemicals

ATP, oxidized ATP (adenosine 5'-triphosphate, periodate oxidized sodium salt), BBG (brilliant blue G), tamoxifen, capsaicin, staurosporine, GdCl<sub>3</sub>, mustard oil, okadaic acid, 18 $\alpha$ -glycerrithinic, carbenoxolone, ruthenium red (RU-2), brefeldin A, reserpine, gibenclamide, verapamil, probenecid, LaCl<sub>3</sub>, tetraethylammonium (TEA), U73122, calmidazolium, HC-03001, capsazepine, and DIDS, were purchased from Sigma Chemical St. Louis, MO, U.S.A.). Fura-2 AM was from Molecular Probes, Dulbecco's modified Eagle's medium (DMEM), fetal calf serum (FCS) and gentamycin were obtained from Gibco (USA).

## Cultured Müller glia

Briefly, chick retina (0.25 retina per well) was dissociated using triple solution, and cells (neurons, glia and progenitors) were seeded over 35 mm culture dishes, 96 well plates or in 15 mm glass coverslip (Marienfeld, Germany) placed in 12 well dishes (Nunc International) in DMEM containing 10% FCS. After 10 days, cell cultures were incubated with 4 mM ascorbic acid for approximately 1.5 h to eliminate neurons, if necessary. After this stage, only glia cells were found, previously confirmed through immunocytochemistry analysis for glial or neuronal markers (Reis et al. 2002). Cultures were subsequently washed with DMEM, and purified glial cultures were obtained at E9C11–15 (cultures prepared from 9-day-old embryos maintained for 11–15 days *in vitro*).

## Dye uptake

Avian Müller cells permeabilization was visualized by the differential uptake of 500 ng/mL propidium iodide (PI) essentially as described before (Freitas et al. 2016; Faria et al. 2016). Briefly, cells were plated in a 24-well (microscopy) or 96-well (fluorescent plate reader) plate (Corning, SP, Brazil), and incubated with P2X7R antagonists, pore forming proteins antagonists or diverse antagonists of intracellular pathways for 10 min, with the exception of 300  $\mu$ M ox-ATP, which was incubated for 50 min. After this initial incubation, 5 mM ATP was added, and the cells were incubated for 25 min, in the presence of antagonists. PI was added during the last 5 min of the ATP incubation. After these procedures, cells were washed, the medium was replaced with extracellular saline solution, and the cells

were imaged by fluorescence microscopy (Nikon, Eclipse TS2000, Tokyo, Japan). Data were analyzed with Image J software, version 4.02 (National Institutes of Health). The positive cells were displayed under red fluorescence, under the same conditions used for the negative control (untreated cells). The spectrofluorometric measurement of dye uptake in avian Müller glial cells was suspended at  $2.5 \times 10^6$  cells/mL in assay buffer composed of 10 mM HEPES, 5 mM KCl, 1 mM MgCl<sub>2</sub>, 1 mM CaCl<sub>2</sub> and 140 mM NaCl (pH 7.4). Antagonists were added to each sample, followed by ATP treatment for 25 min. Plates were incubated at 37 °C for 30 min., and the cellular accumulation of PI was determined by measuring the fluorescence with a Molecular Devices SpectraMax M5 fluorescent plate reader (excitation wavelength 530 nm; emission wavelength 590 nm).

### Electrophysiology

Ionic currents were recorded using a whole-cell configuration (patch-clamp technique) from avian Müller cells in culture, with an Axopatch-1D amplifier (Axon Instruments, San Mateo, CA, USA). All recordings were performed at 37 °C. Cells were transferred to a chamber mounted on a microscope stage (Nikon, Eclipse TS2000, Tokyo, Japan). Patch pipettes were pulled from IBBL borosilicate glass capillaries (1.2 mm, inner filament; World Precision Instruments, New Haven, CT, USA). A high-resistance seal (1–10 G $\Omega$ ) was established by gentle suction, and the circumscribed cell membrane was disrupted using additional suction. Currents obtained in the presence of agonist were not corrected for leakage, because it was negligible; in the absence of agonist, currents were less than 0.15% of the maximal agonist induced currents. Currents were recorded after 5 to 10 min of dialysis of internal solutions. Recordings were included for analysis, only when the current and membrane conductance returned to within 1 to 5% of the control values after agonist washout. This procedure prevented the possibility of considering artefactual current increase through seal leakage or cell dialysis. The holding potential was adjusted to –60 mV, except for the voltage ramps, which was –80 mV. The series resistance was 6 to 10 M $\Omega$  for all experiments, and no compensation was applied for currents smaller than 400 pA. Above this level, series resistances were 80% compensated. The experiments in which the series resistance increased substantially during the measurement process were discarded. Cell capacitance ( $10.53 \pm 3.31$  pF;  $n = 148$ ) was measured by applying a 20 mV hyperpolarizing pulse, starting from a holding potential of –20 mV. The capacitive transient was then integrated and divided by the amplitude of the step voltage (20 mV). Cells with access resistance ( $R_a$ ) values higher than 25 M $\Omega$  or varying by more than 20% during the experiment, were discarded.

Ionic currents were filtered with a current frequency of 5 kHz (8-pole Bessel filter), digitized at 20–50 kHz using a Digidata 1320 interface (Axon Instruments, Palo Alto, CA), and acquired with a personal computer using pClamp 9 software package. Reversal potentials were then depicted directly from the current-voltage plots.

Relative current was defined as the ratio between the peak amplitude of the ionic current and the cell capacitance. Maximal response was defined as the response to ATP alone. All other recordings of antagonists in the presence of ATP were normalized, in relation to this maximal value.

### Drug application

Experiments were performed under perfusion (RC-24 chamber, Warner Instrument Corporation, Hamden, USA), and under constant flow of external solution to confirm the data obtained through the application of micropipette. Whole-cell patch-clamp recordings were performed using avian Müller glia cells, which were bathed in an external solution containing the following (mM): 150 NaCl, 5 KCl, 1 MgCl<sub>2</sub>, 1 CaCl<sub>2</sub>, and 10 HEPES, pH 7.4. The pipette solution contained the following (mM): 150 KCl, 5 NaCl, 1 MgCl<sub>2</sub>, 10 HEPES, and 0.1 EGTA, pH 7.4, at room temperature.

### Single cell calcium imaging

Free intracellular calcium levels ( $[Ca^{2+}]_i$ ) were measured in avian Müller cells in culture adapting the protocol from (De Melo Reis et al. 2011), essentially described in (Freitas et al. 2016). Briefly, glia cells in culture were loaded for 40 min with 5  $\mu$ M Fura-2/AM (Molecular Probes), 0.1% fatty acid-free bovine serum albumin (BSA), and 0.02% pluronic acid F-127 (Molecular Probes) in Krebs solution (132 mM NaCl, 4 mM KCl, 1.4 mM MgCl<sub>2</sub>, 2.5 mM CaCl<sub>2</sub>, 6 mM glucose, 10 mM HEPES, pH 7.4), in an incubator with 5% CO<sub>2</sub> and 95% atmospheric air at 37 °C. After a 10-min post-loading period at room temperature in Krebs solution, to obtain a complete hydrolysis of the probe, 15 mm coverslip (Marienbad, Germany) with the cells was mounted on a chamber in a PH3 platform (Warner Instruments, Hamden, CT) on the stage of an inverted fluorescence microscope (Axiovert 200; Carl Zeiss). Cells were then continuously perfused with Krebs solution and stimulated with different solutions (ATP alone or in the presence of selected drugs). Solutions were added to the cells by a fast-transition system that allowed drugs to reach the cells in less than 8 s. The variations in  $[Ca^{2+}]_i$  were evaluated by quantifying the ratio of the fluorescence emitted at 510 nm following alternate excitation (750 milliseconds) at 340 and 380 nm, using a Lambda DG4 apparatus (Sutter Instrument, Novato, CA) and a 510 nm long-pass filter (Carl Zeiss) before fluorescence acquisition with

a 40X objective and a Cool SNAP digital camera (Roper Scientific, Trenton, NJ). Acquired values were processed using the MetaFluor software (Universal Imaging Corp., West Chester, PA). Values for Fura-2 fluorescence ratio were calculated based on a cut-off of 10% increase in the  $[Ca^{2+}]_i$  level induced by the stimulus.

### Data analysis

Fluorescence was normalized for the maximal fluorescence value using Microsoft Excel, and plotted the results using the GraphPad Prism version 3.0 (San Diego, CA, U.S.A). Data were expressed as mean  $\pm$  SD (standard deviation), as indicated in the text. To evaluate whether samples followed Gaussian distribution and Pearson normality, tests were used. If case data followed a Gaussian distribution, an analysis of variance (ANOVA) was applied followed by Tukey's test. A bicaudal  $p < 0.05$  was considered significant.

Area under the curve was calculated using Origin 6.1 software (OriginLab Corporation, Washington, USA). Maximal response was defined as the response to ATP alone. All other recordings of antagonists in the presence of ATP were normalized, in relation to this maximal value.

## Results

### Intracellular signaling associated to P2X7R macroscopic currents

Intracellular calcium mobilization was evaluated upon addition of ATP in avian Müller glia cells in culture, showing a typical flat appearance (Fig. 1a). Figure 1b show the same microscope field under fura-2 fluorescence in single cell calcium imaging experiments. Dose response curve for ATP 0.01 mM (C), 0.1 mM (D), 0.5 mM (E), 1 mM (F) and 5 mM (G) show that few cells were activated by 0.01–0.1 mM ATP (arrows), but at milimolar concentrations of ATP, the majority of glia cells were responsive. Quantification of these results are shown in Fig. 1h for at least 720 analyzed glial cells ( $n = 4$ ). The activation of the majority of Müller glia cells by milimolar ATP suggests that P2X7R is involved.

We used selective agents to rule out participation of other P2X and P2Y members in calcium mobilization stimulated by ATP. In Fig. 2a–i, Müller cells treated with 1 mM ATP (Fig. 2c), or in the presence of the reactive Blue-2 (RB-2, Fig. 2d), a general P2YR blocker; suramin, a general P2R blocker (Fig. 2e) and Pyridoxalphosphate-6-azophenyl-2',4'-

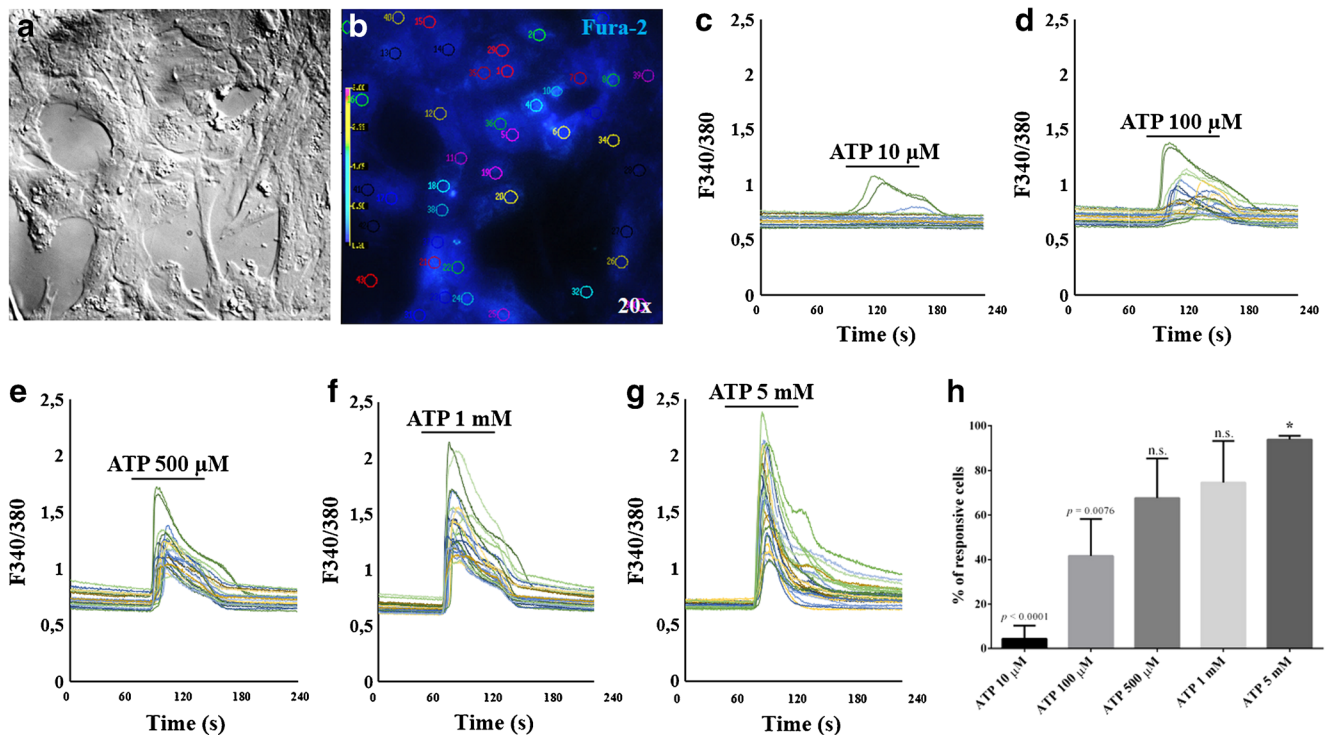


**Fig. 1** ATP-induced calcium shifts in avian Müller glial cells. **(a)** Müller cells in culture prepared from embryonic avian retina showing a typical flat appearance. **(b)** The same microscope field is shown under fura-2 fluorescence in single cell calcium imaging experiments. Dose response curve for **(c)** ATP 0.01 mM, **(d)** 0.1 mM, **(e)** 0.5 mM, **(f)** 1 mM and **(g)** 5 mM on Müller glia. Few cells were activated by 0.01 mM ATP (at a

340/380 nm excitation ratio), but 0.5 mM or higher concentrations of ATP induced responses in most evaluated cells. **(h)** Percentage of responsive glial cells activated by ATP (0.01–5 mM). At least 720 cells were analyzed ( $n = 4$ ). Experiments were performed from different cultures prepared on at least 4 different days. \*Significance is for each comparison value is shown in **(h)**

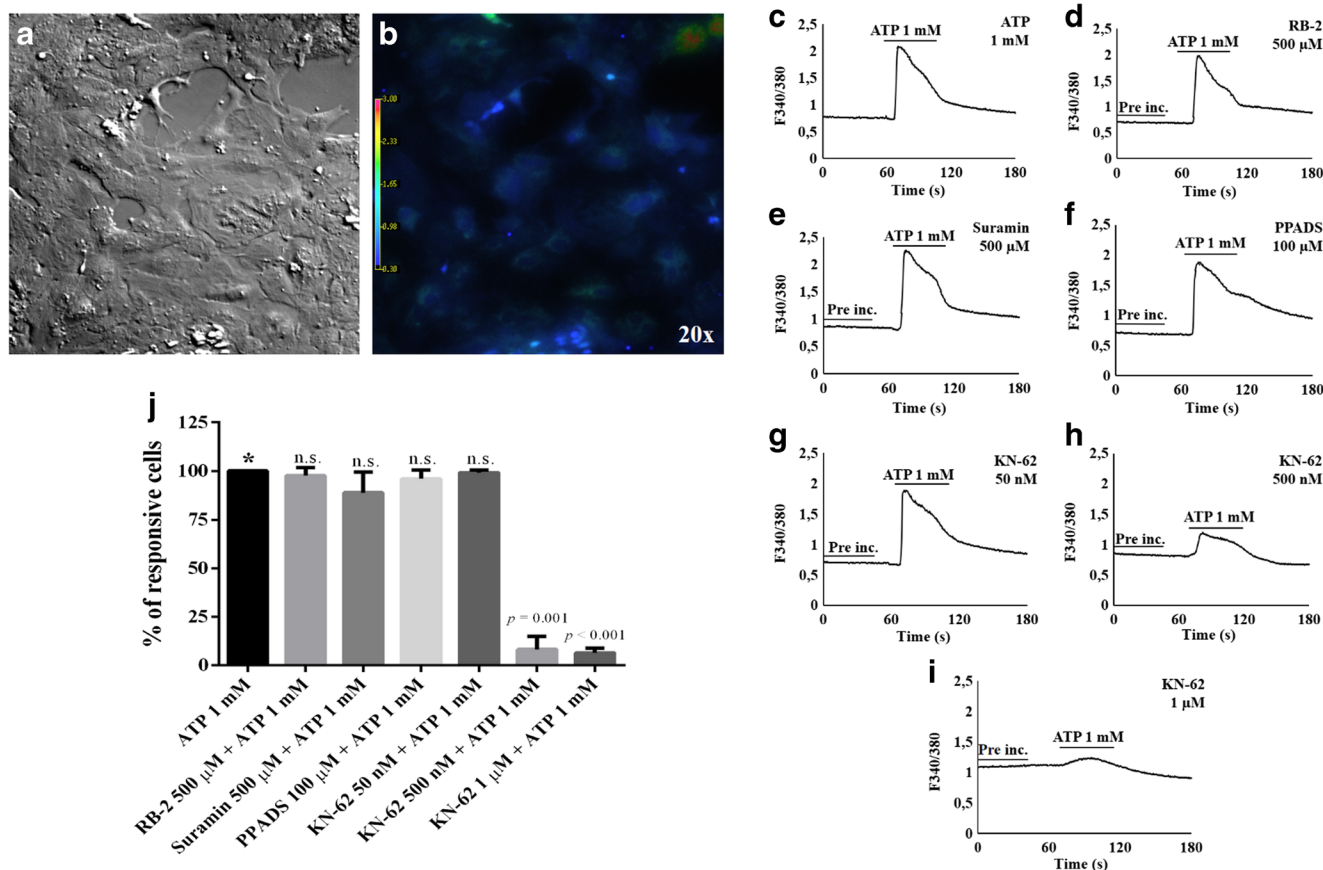


**Fig. 2** ATP-induced calcium shifts in the presence of selective antagonists. (a) Müller cells in culture showing a typical flat appearance. (b) The same microscope field is shown under fura-2 fluorescence. Cells were stimulated with (c) ATP 1 mM alone or under preincubation of (d) RB-2500 μM, (e) Suramin 500 μM, (f) PPADS

100 μM, (g) KN-62 50 nM, (h) 500 nM or (i) 1 μM. (j) Quantification data illustrates percentage of responsive cells. At least 2100 cells were analyzed ( $n = 4$ ). Experiments were performed from different cultures prepared on at least 4 different days. \*Significance is for each comparison value is shown in (j)

disulfonic acid (PPADS), a general P2XR blocker (Fig. 2f). As expected for P2X7R, there was no inhibition (Fig. 2j) for calcium shifts induced by ATP in the presence of these agents. On the other hand, KN-62 fully reduced ATP-induced effect in a dose dependent manner (Fig. 2g-i). Quantification of data related to the antagonist's effects in the presence of ATP is shown (Fig. 2j).

In order to evaluate the participation of other P2XR in the ATP-induced calcium shift in Müller cells (Fig. 3a-p), other selective antagonists were also used to compare with ATP (Fig. 3c); 10 μM NF770, a P2X2R antagonist (Fig. 3d); MRS2578, a P2Y6 antagonist (Fig. 3e), 10 μM 5-BDBD, a P2X4R antagonist (Fig. 3f); TNP-ATP, a P2X1R antagonist (Fig. 3g); AR-C118925, a P2Y2R antagonist (Fig. 3h) or MRS 2179, a P2Y1R antagonist (Fig. 3i). Neither antagonists inhibited ATP induced  $Ca^{2+}$  mobilization (Fig. 3m), except for MRS2179, which inhibited in turn of 40% of ATP response (Fig. 3i).

We also confirmed the participation of P2X7R in the ATP-induced  $Ca^{2+}$  shift, when BzATP (100 μM) was added

(Fig. 3j) and its effect was inhibited by the selective P2X7R antagonist, A740003 (Fig. 3k). Quantification of data related to the effects upon the antagonists in calcium shift induced by ATP (Fig. 3l) or BzATP (Fig. 3m) is shown.

Müller cells treated with increasing ATP concentrations induced macroscopic currents in a dose dependent manner (Fig. 4a and b). The  $EC_{50}$  value measured for ATP effect was 528.5 nM (Fig. 4b). Treatment with ATP for 1 and 3 h of continuous exposition did not induce LDH release (data not shown). We confirmed P2X7R participation as the major component of these ionic currents using P2X7R agonist, BzATP (300 μM), which effect was blocked with the P2X7R antagonist oxidize ATP (oATP, Fig. 4c). Since ATP was applied in a short-term pulse (1 min), this could in theory hamper the characterization between other members of the P2X7 family based on the kinetic properties of macroscopic currents. However, this protocol was used because it show a similar pharmacological profile (Supplemental Fig. 1A) exhibited when ATP was applied for a longer period (5 min) (Supplemental Fig. 1B). Addition of a general

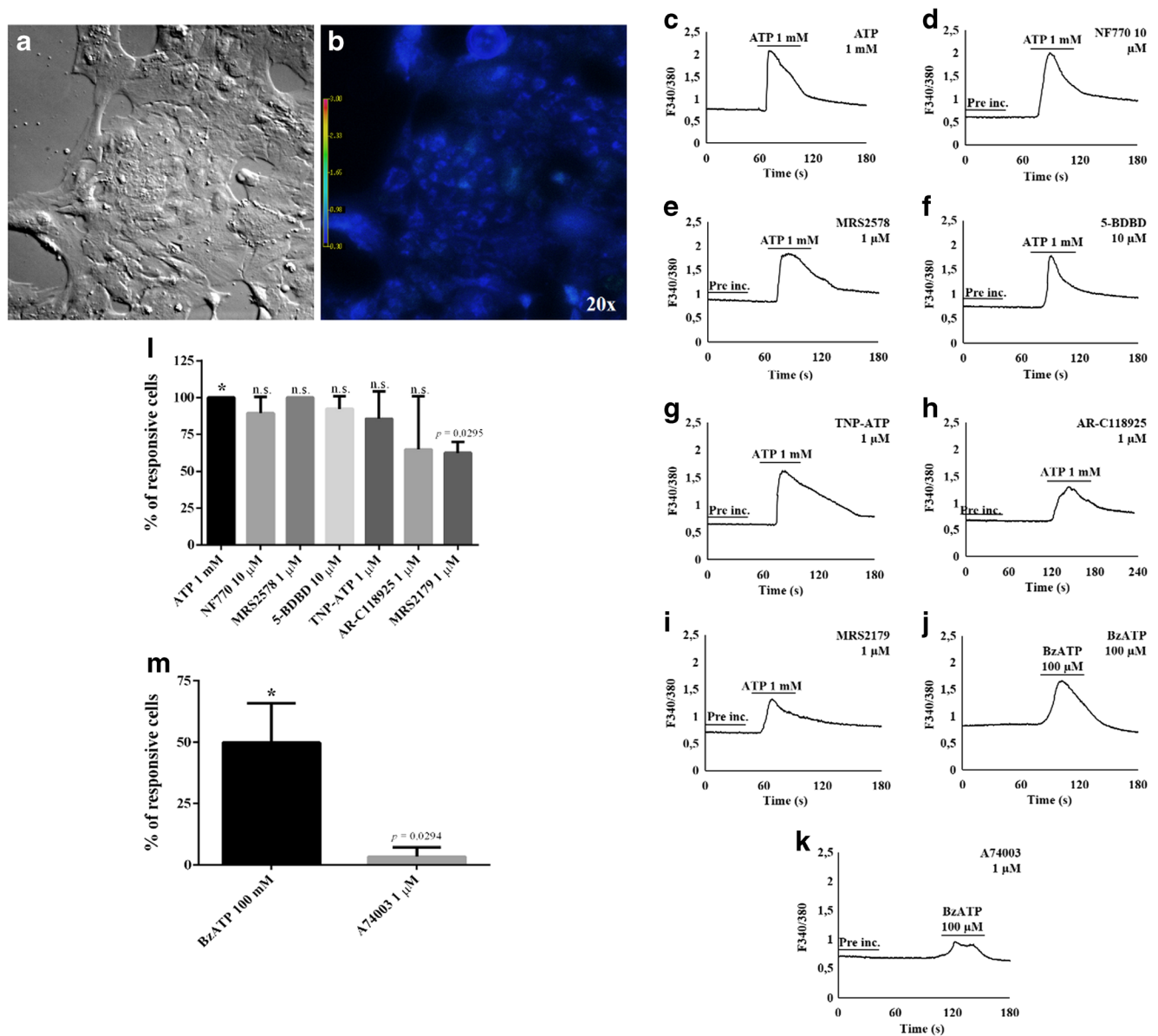


**Fig. 3** ATP or BzATP-induced calcium shifts in the presence of selective antagonists. **(a)** Müller cells in culture showing a typical flat appearance. **(b)** The same microscope field is shown under fura-2 fluorescence. Cells were stimulated with **(c)** ATP 1 mM alone or under preincubation of **(d)** NF770 10 μM, **(e)** MRS2578 1 μM, **(f)** 5-BDBD 10 μM, **(g)** TNP-ATP 1 μM, **(h)** AR-C118925 1 μM or **(i)** MRS2179 1 μM. Cells were also stimulated with **(j)** BzATP 100 μM or under preincubation of **(k)** A74003

1 μM. Quantification data illustrates percentage of responsive cells activated by **(l)** ATP 1 mM alone or in the presence of selective antagonists, or **(m)** BzATP 100 μM alone or in the presence A74003 1 μM. At least 2500 cells were analyzed ( $n = 4$ ). Experiments were performed from different cultures prepared on at least 4 different days. \*Significance is for each comparison value is shown in **(l)** and **(m)**

P2Y receptor antagonist, Reactive Blue-2 (RB-2); a selective P2X2R antagonist, NF770; a selective P2X4R antagonist, 5BDBD or the P2X1R and P2X3R antagonist TNP-ATP, these drugs had no effect on ATP-induced current in both protocols with distinct time of ATP treatment (Supplemental Fig. 1). In addition, selective P2X7R antagonists (AZ10606120 and A740003) blocked ATP induced macroscopic currents in both protocols (Supplemental Fig. 1).

Avian Müller cells treated with 5 mM ATP induced typical macroscopic currents (Fig. 5a). Addition of a P2X7R antagonist, 300 μM oATP, fully inhibited ATP-induced currents (Fig. 5b). Based in previous reports from our group (Faria et al. 2016, 2010), and in order to gain knowledge on P2X7R signaling in avian Müller glia, cells were treated with antagonists of intracellular pathways or large conductance pore blockers. As shown, 10 μM PD98059, an extracellular signal-regulated kinase (ERK) inhibitor, or 10 μM U73122, a

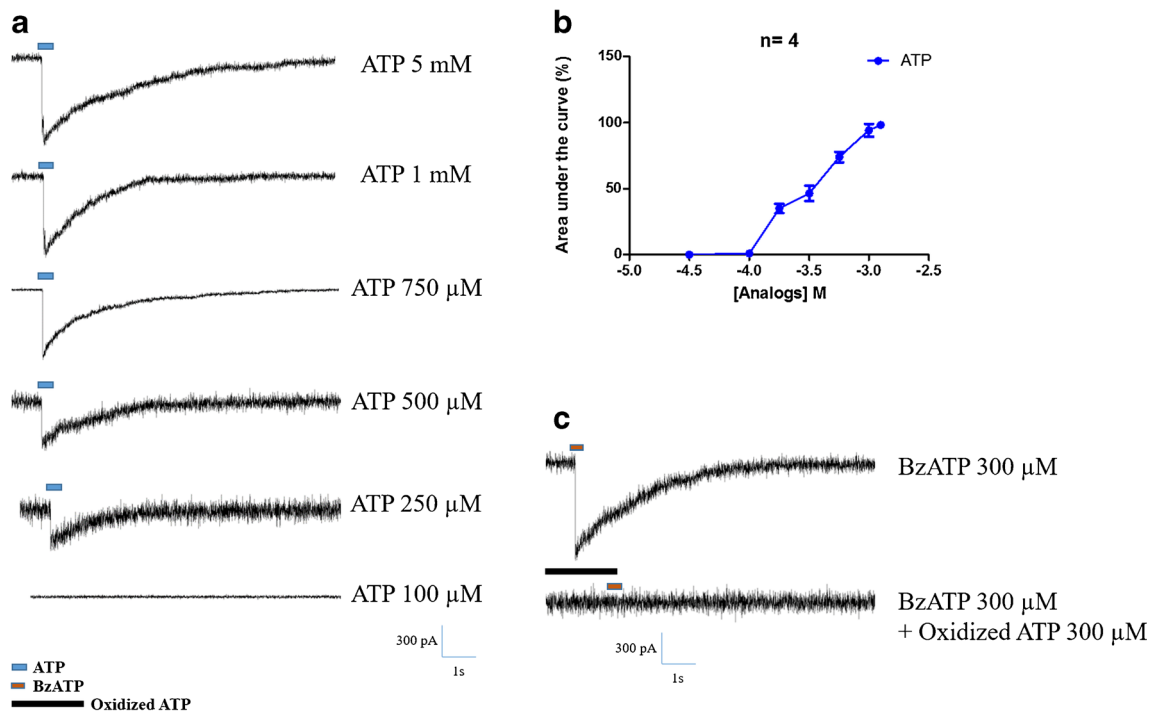


**Fig. 4** ATP-induced macroscopic currents in avian Müller glial cells. **(a)** Electrophysiological recording of macroscopic ionic currents induced by ATP concentrations at 37 °C. **(b)** Quantification of the area under the curve of the recordings obtained after the treatment with ATP 0.1 mM, 0.25 mM, 0.5 mM, 0.75 mM, 1 mM and 5 mM on Müller glia. **(c)**

Electrophysiological recording of Müller glia activated with BzATP 300  $\mu$ M preincubated with Oxidized ATP 300  $\mu$ M for 1 h or not. Experiments were performed from different cultures prepared on at least 4 different days ( $n = 4$ )

phospholipase C inhibitor did not reduce ATP-induced currents (Fig. 5c and d), respectively. However, addition of 10  $\mu$ M SB203580, a MAPK p38 inhibitor, or 10  $\mu$ M calmidazolium, blocker of CAMKII, or 10  $\mu$ M chelerythrine as well as 10  $\mu$ M RO-82220, PKC inhibitors, or 1  $\mu$ M wortmannin, a PI3-K inhibitor, they all reduced ATP-induced currents (Fig. 5e-i). On the other hand, incubation of 100  $\mu$ M carbenoxolone (CBX), a connexin hemichannel uncoupler, or 1 mM probenecid, a pannexin-1 hemichannel blocker, or 10  $\mu$ M okadaic acid, a plasma VDAC inhibitor, showed no effects on ATP-induced currents (Fig. 3j-l). Finally, addition of 10  $\mu$ M ruthenium red (RU-2), a general TRPV antagonist, blocked ATP action (Fig. 5m). Quantification of data related to the antagonist's effects upon currents induced by ATP is shown (Fig. 5n and o). Among all inhibitors of large conductance channels tested, only RU-2 reduced ionic currents promoted by ATP (Fig. 5n). On the other hand, addition of CBX, probenecid, mefloquine (a pannexin-1 inhibitor), 4, 4'-diisothiocyano-2,2'-disulfonic acid stilbene (DIDS, an anionic channel blocker), HC-03003 (a TRPA1 antagonist), GdCl<sub>3</sub><sup>+</sup> (a maxi anion blocker) or okadaic acid, they all had no effect on ATP-induced ionic currents (Fig. 5o).

A dose-dependent antagonist action of the drugs used for inhibiting P2X7R is shown (Fig. 6). All ionic recordings are representative of experiments with ATP treatment preincubated with blockers in the concentrations of 1 nM, 1  $\mu$ M and

100  $\mu$ M, as described. Calmidazolium caused a prominent inhibition in concentrations higher than 1  $\mu$ M (Fig. 6a-c). SB203580 (Fig. 6d-f), wortmannin (Fig. 6g-i) and BBG (Fig. 6j-l) produced a more potent inhibition with a reduction superior to 60% at 1  $\mu$ M. Ru-2 (Fig. 6m-o) had a lower inhibition compared to PKC inhibitors, Ro-8220 (Fig. 6p-r), chelerythrin (Fig. 6s-u) and calphostin C (Fig. 6v-y). Dose-response curves for SB203580, wortmannin, calmidazolium or RU-2 against ATP-induced ionic currents produced IC<sub>50</sub> values of 0.266  $\mu$ M, 3.717  $\mu$ M, 0.095  $\mu$ M and 4.398  $\mu$ M, respectively (Fig. 6w). The P2X7R antagonist BBG exhibited an IC<sub>50</sub> value of 109.5 nM (Fig. 6w). All PKC antagonists also efficiently inhibited ATP-induced currents with IC<sub>50</sub> values of 0.34  $\mu$ M (calphostin C), 0.101  $\mu$ M (Ro-8220) and 0.812  $\mu$ M (chelerythrine) (Fig. 6z). No antagonists tested interfered in the activation (Supplemental Fig. 2A) or deactivation time (Supplemental Fig. 2B) of the P2X7R function, they only affect the amplitude of response.

Intracellular calcium mobilization was also evaluated upon addition of ATP alone or in the presence of intracellular signaling pathway blockers. ATP evoked a shift in the intracellular calcium concentration as shown (Fig. 7a). Addition of 500 nM BBG partially inhibited Ca<sup>2+</sup> increase induced by ATP (Fig. 7b). Addition of 10  $\mu$ M RU-2 almost extinguished ATP-induced calcium increase (Fig. 7c), while 10  $\mu$ M calmidazolium, 1  $\mu$ M wortmannin or 10  $\mu$ M RO-318220

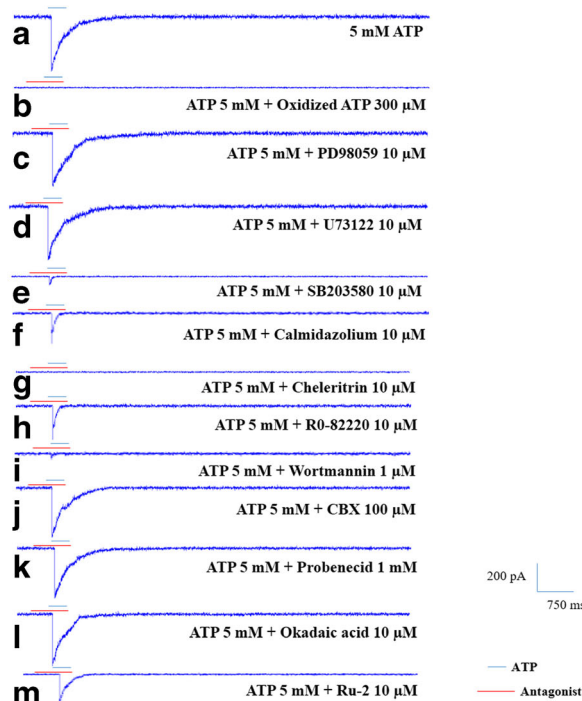
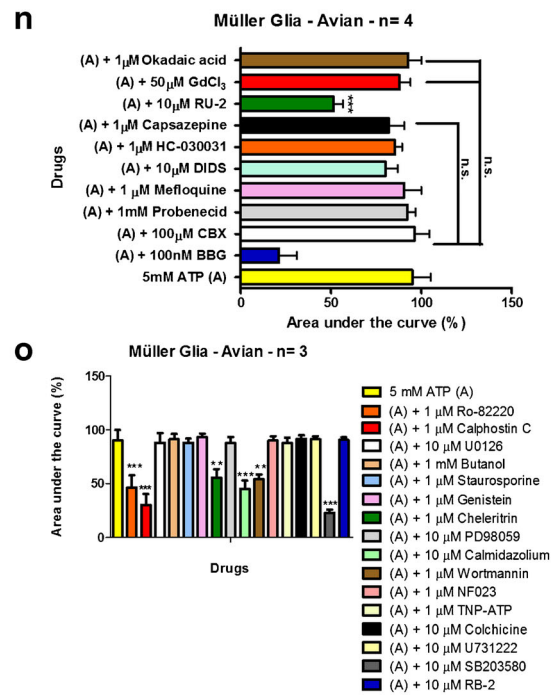


**Fig. 5** ATP-induced ionic currents on avian Müller glial cells. Pharmacological profile of the ATP-induced currents in whole cell experiments at 37 °C. Macroscopic current traces induced by ATP (a). ATP-induced current were also recorded in the presence of blockers as oxidized ATP (b), PD98059 (c), U73122 (d), SB203580 (e), calmidazolium (f), colchicine (g), Ro-8220 (h), wortmannin (i),



carbenoxolone (CBX) (j), probenecid (k), okadaic acid (l) and ruthenium red (Ru-2) (m). All compounds incubated for 10 min before addition of ATP. (n) Bar graph of ATP-induced currents in the presence of large conductance pore blockers, or (o) in the presence of intracellular signaling pathway blockers. Experiments were performed in at least in 5 distinct cells, from different cultures prepared on at least 3 different days ( $n = 3$ )

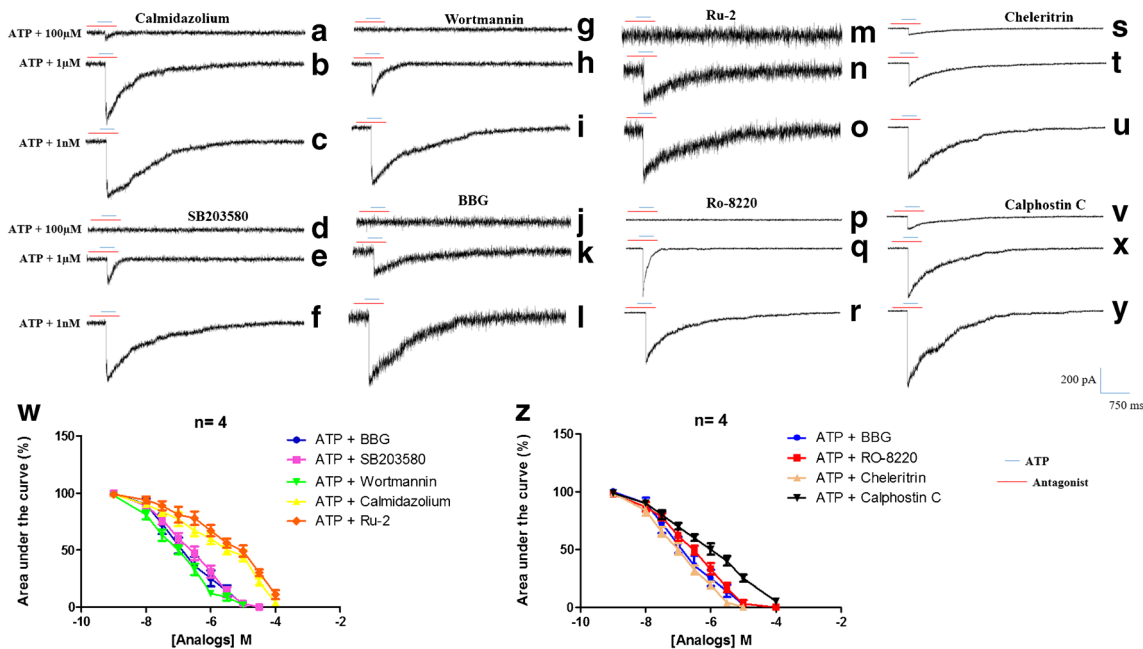


**Fig. 6** Dose response curves for ATP-induced currents in Müller cells in culture by selective antagonists. (a-y) Representative electrophysiological recordings of experiments using the antagonists of intracellular signaling and Ru-2 with activity against P2X7R ionic currents. All represented antagonists are in the presence of ATP and we used 3 representative recordings. (w) Dose response curves for ATP-induced currents in the

presence of BGG, SB203580, wortmannin, calmidazolium or ruthenium-2 (Ru-2); (z) or in the presence of BGG, or selective PKC antagonists Ro-8220, Chelerythrin or Calphostin. The concentrations of the added blockers are given in the text. Data represent the quantification of 4 independent experiments ( $n = 4$ )



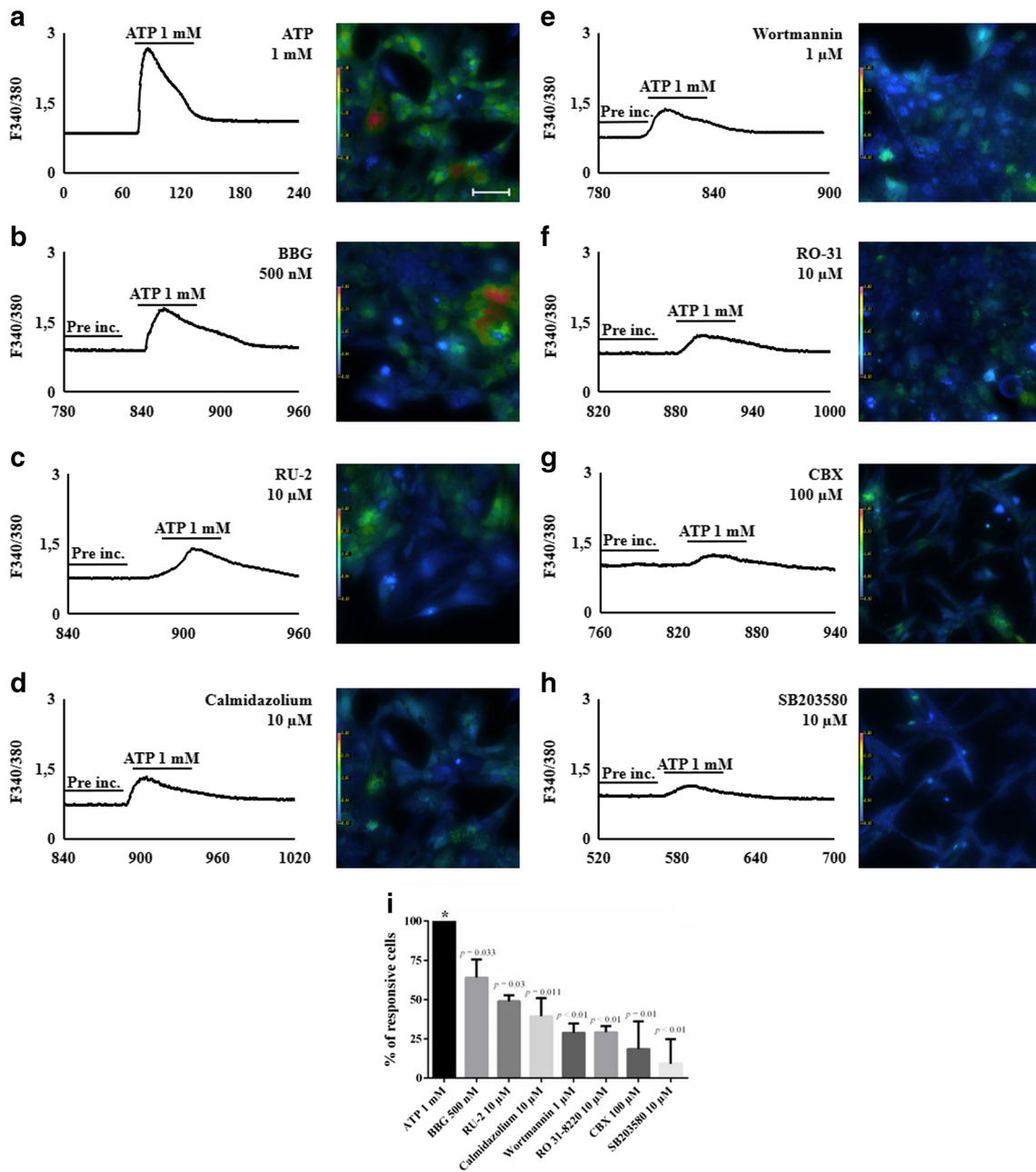


**Fig. 7** ATP-induced calcium shifts in the presence of diverse antagonists. (a) Typical calcium imaging traces of fluorescence emission (340/380 nm excitation ratio) of a representative glial cell activated by ATP 1 mM alone or in the presence of (b) BBG 500 nM, (c) RU-2 10 μM, (d) Calmidazolium 10 μM, (e) Wortmannin 1 μM, (f) RO-318220 10 μM,

(g) CBX 100 μM, or (h) SB203580 10 μM in avian Müller glial cells in culture (inset). (i) Quantification data illustrates percentage of responsive cells activated by ATP in each condition. At least 1500 cells were analyzed ( $n = 3$ ). A. 50 μm scale bar. \*Significance is for each comparison value is shown in (i)

decreased ATP induced calcium mobilization (Fig. 7d-f). Surprisingly, 100 μM CBX also potently inhibited ATP-induced calcium currents (Fig. 7g). In addition, the presence of 10 μM SB203580 almost fully inhibited  $Ca^{2+}$  mobilization promoted by ATP (Fig. 7h). A general inhibition profile with the respective potency order is shown in Fig. 7i. As illustrated, MAPK antagonists and CBX were the most potent inhibitors among the blockers used.

ATP-induced dye uptake was also measured in Müller glial cells using fluorescence microscopy and a fluorescent plate reader. As expected, negative control did not show dye uptake (Fig. 8a), in contrast to positive control (Fig. 8b), where there was maximal dye uptake. Addition of 5 mM ATP for 20 min promoted a PI uptake (Fig. 8c), which was inhibited by 100 nM BBG (Fig. 8d). oATP also inhibited P2X7R mediated effect (Fig. 8e). Treatment with large conductance pore

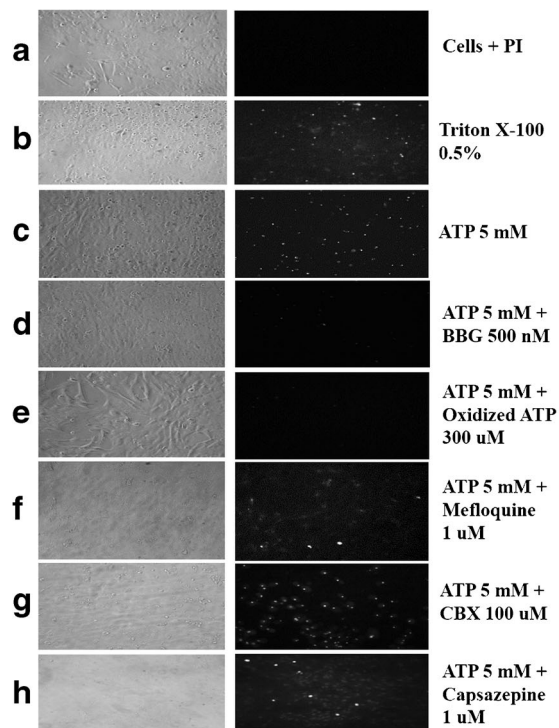
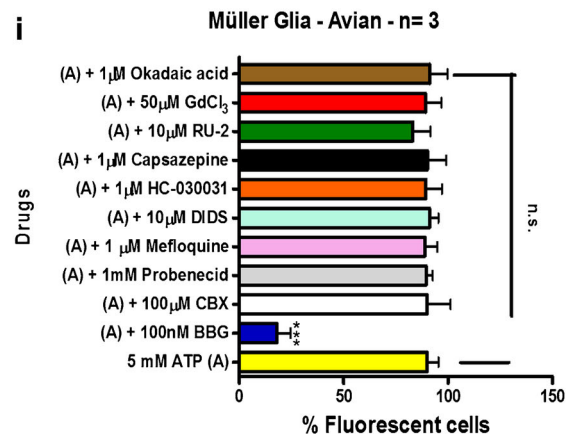


**Fig. 8** ATP induced PI uptake in avian primary Müller glial cells did not inhibit by pore forming proteins antagonists. *Left panels* are phase contrast images while *right panels* are fluorescence showing PI uptake. Controls represent (a) no treated cells or (b) treated with detergent to disrupt cell membrane. (c) PI uptake assay upon treatment of ATP 5 mM for 20 min at 37 °C, or in the presence of (d) BBG 500 nM, (e) Oxidized ATP 300 μM, (f) Mefloquine 1 μM, (g) CBX 100 μM, (h) Capsazepine 1 μM. (i) Bar graph representing PI uptake induced by



inhibitors did not inhibit ATP-induced dye uptake (Fig. 8f-i). In relation to the intracellular signaling pathways, calmidazolium (Fig. 9b and i), a CAMKII inhibitor, PD98059, a MEK inhibitor (Fig. 9c and i), TNP-ATP, a P2X inhibitor (Fig. 9d and i) and U73122, a PLC inhibitor (Fig. 9e and i), did not inhibit P2X7R-mediated dye uptake. Similarly, other antagonists also had no effect on ATP-induced dye uptake, such as U0126 (general PLC inhibitor), butanol (general PLD inhibitor), staurosporine (protein serine and tyrosine kinase antagonist), genistein (tyrosine kinase inhibitor), NF-023 (P2X1 and P2X3 antagonist) and reactive blue 2 (RB-2) (general P2Y antagonist), as shown in Fig. 9i. In contrast, PKC, MAPK, PI3K inhibitors or the microtubule antagonist, all reduced ATP-induced dye uptake (Figs. 10f-g and 9i). However, Ru-2, or calmidazolium, a CAMKII inhibitor did not interfere with the ATP-induced dye uptake. The  $IC_{50}$  values to SB203580 (a MAPK inhibitor), wortmannin (a PI-3 K inhibitor) or colchicine (a microtubule inhibitor) treatment were 0.198 μM, 0.164 μM and 0.179 μM, respectively (Fig. 10a). In addition, PKC antagonists exhibited  $IC_{50}$  values of 0.257 μM, 0.049 μM and 0.129 μM to Ro-8220, chelerythrine and calphostin C, respectively (Fig. 10b). We

ATP 5 mM alone (20 min stimulus) or in the presence of P2X7 blockers and pore forming proteins blockers, which were incubated for 10 min before addition of ATP. The concentrations of the added blockers are given in the text. \*Significantly different from the control at  $p < 0.05$ . \*\*Significantly different from ATP at  $p < 0.05$ . Experiments were performed in triplicate from at least three independent cultures performed on different days ( $n = 3$ )

excluded a hypothetical toxicity induced by antagonists after incubating them in the same concentration and time used in the presence of ATP. As observed in the supplementary Fig. 3, no toxicity was noticed promoted by antagonists alone.

## Discussion

Here we studied the properties of the avian Müller glia P2X7 receptor (P2X7R) using multiple approaches, as electrophysiology, single cell  $Ca^{2+}$  imaging, and dye uptake assay in purified glia culture. Previous patch-clamp studies in human Müller glia show that these cells express P2X7R, as BzATP was the most effective agonist to evoke large inward currents, abolished by P2X antagonists (Pannicke et al. 2000). Our data confirm that ATP (or BzATP) evoked large inward currents in patch-clamp studies, while addition of P2X7R antagonist such as brilliant Blue G (BBG) or oxidized ATP (oATP), abolished these currents (Fig. 2). Curiously, the  $IC_{50}$  for BBG (109.5 nM) to P2X7R inhibition is similar when compared to other species, such as 10 nM for rat P2X7 and 200 nM for human P2X7 (Fig. 4w) (Bartlett et al. 2014; Donnelly-Roberts et al. 2009).

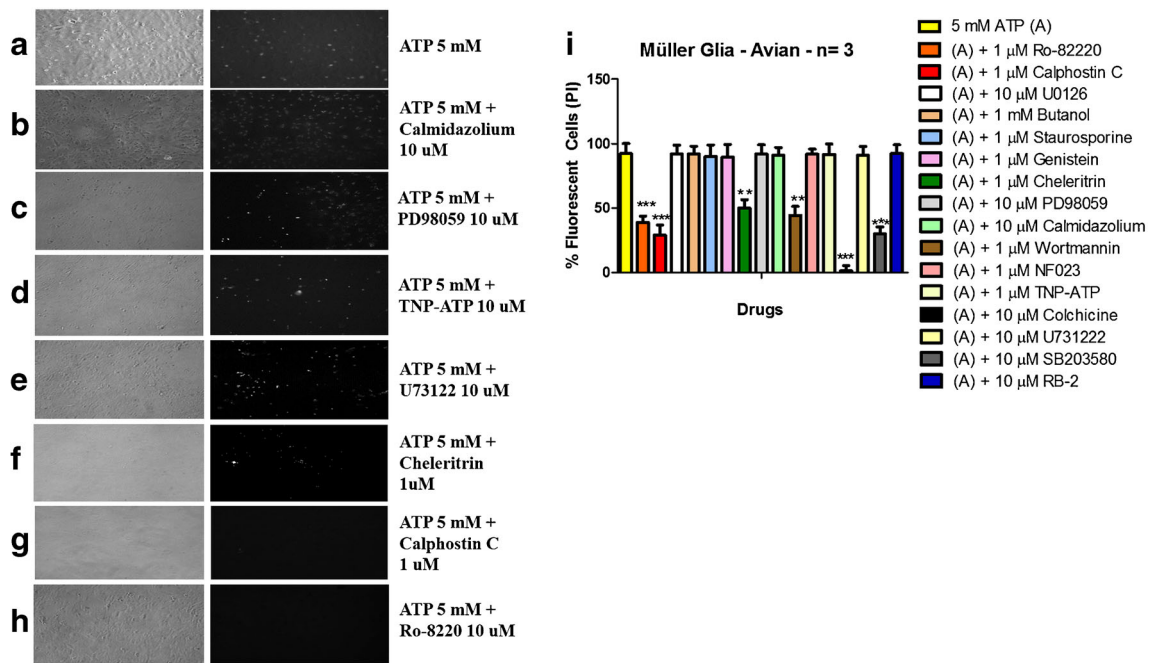


**Fig. 9** ATP induced PI uptake in avian primary Müller glial cells is affected by intracellular signaling antagonists. *Left panels* are phase contrast images while *right panels* are fluorescence showing PI uptake. (a) PI uptake assay upon treatment of ATP 5 mM for 20 min at 37 °C, or in the presence of (b) Calmidazolium 10 μM, (c) PD98059 10 μM, (d) TNP-ATP 10 μM, (e) U73122 10 μM, (f) Chelerythrine 1 μM, (g) Calphostin C 1 μM, (H) Ro-8220 10 μM. (I) Bar graph representing PI

uptake induced by ATP alone 5 mM (20 min stimulus) or in the presence of P2X7 blockers and intracellular signaling pathway blockers, which were incubated for 10 min before addition of ATP. The concentrations of the added blockers are given in the text. \*Significantly different from the control at  $p < 0.05$ . \*\*Significantly different from ATP at  $p < 0.05$ . Experiments were performed in triplicate from at least three independent cultures performed on different days ( $n = 3$ )

The role of P2X7R in the ATP-induced  $Ca^{2+}$  mobilization was characterized by BzATP response, inhibited by A740003 (Fig. 10). Additionally, general or selective P2XR antagonists (Figs. 2 and 3) did not reduce ATP response. In relation to P2YRs, general antagonists as RB-2 did not inhibit, however the selective P2Y1 antagonist diminished the ATP effect. Although this result indicates that P2Y1R has a role in the ATP response, P2X7R inhibition with KN-62 almost fully inhibited ATP-induced  $Ca^{2+}$  shift (Fig. 9j). Thus, the P2Y1R may not be essential in the  $Ca^{2+}$  current induced by ATP, but this deserves further investigation.

It is worth to mention that Müller cells display a range of intensity and shape of currents suggesting that other purinergic receptors might be activated by ATP. It is known that Müller and bipolar retinal cells proliferate at early embryonic stages upon activation of P2Y1 receptors coupled to signaling pathways such as phospholipase C, PKC and MAP kinases (Sanches et al. 2002). However, intracellular pathways have a role in the modulation of  $Ca^{2+}$  signaling through P2X7R in Müller cells in culture, as done recently for astrocytes (Faria et al. 2016) and macrophages (Faria et al. 2010).

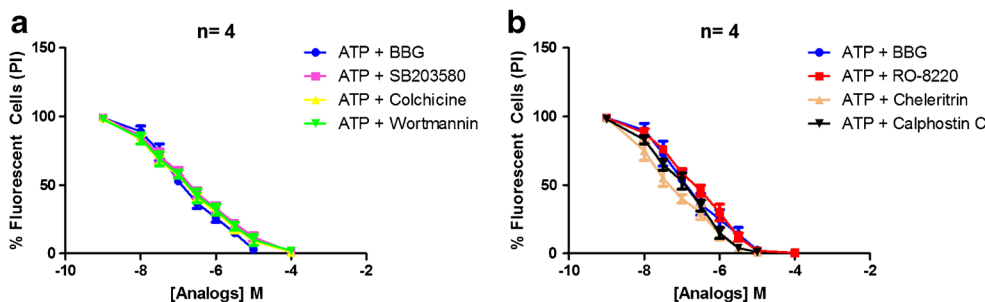


**Fig. 10** ATP induced PI uptake in avian primary Müller glial cells is affected by intracellular signaling antagonists. (a) Dose-response graph representing PI uptake induced by ATP 5 mM alone (20 min stimulus) in function of MAPK, microtubule and PI-3 K blockers, which were incubated for 10 min before addition of ATP. (b) Dose-response graph

representing PI uptake induced by ATP 5 mM alone (20 min stimulus) in function of PKC blockers, which were incubated for 10 min before addition of ATP. The concentrations of the added blockers are given in the text. Experiments were performed in triplicate from at least three independent cultures performed on different days ( $n = 3$ )

Recent data have confirmed a role for P2X7R in health and disease for Müller glia (Tewari and Seth 2015; Ancasi et al. 2013) and retinal neurons (Niyadurupola et al. 2013), but it is still a matter of controversy about how the mechanism operates on pore-dilation transition of the cation-conducting pore from 7 Å up to 40 Å (Volonte et al. 2012; Yan et al. 2010; Faria et al. 2010, 2005). Our data from electrophysiology point to the involvement of MAPK, PI3K, CAMKII, microtubules or PKC in the modulation of ATP-induced ionic current in Müller glia. ATP induced  $\text{Ca}^{2+}$  influx was partially inhibited by oATP or BBG, and totally inhibited by blockers of other pores such as TRPs or connexin hemichannel. Additionally, MAPK, PKC, PI3K or CAMKII inhibitors are also involved in the modulation of intracellular calcium signaling. Finally, ATP induced 80–90% of dye uptake in Müller glia cells, while oxidized ATP (oATP), BBG or A740003 inhibited this effect. In Table 1, we listed and compared the proteins with antagonistic activity for ionic currents, intracellular calcium mobilization and pore formation, allowing the identification of possible key proteins regulating each P2X7R function measured. In particular, MAPK antagonist (SB203580) greatly attenuated ATP-induced  $\text{Ca}^{2+}$  internalization (Fig. 5g and h). Indeed, BBG inhibited p38 MAPK activation through selective P2X7 in a recent work (Zou et al. 2016), while BzATP reversed this treatment. In addition, P2X7R was shown to mediate actin reorganization and membrane blebbing in macrophages via p38 MAPK, while p38 inhibitors SB202190 and SB203580 attenuated ATP/BzATP-induced structural actin reorganization (Diaz-Hernandez et al. 2008). Therefore, inhibition of MAPK activation seems to control P2X7-dependent intracellular behavior.

PI3K is a master regulator of the structural cells of the nervous system. Inhibition of PI3K abrogates P2X7R negative effects on axon growth and branching of hippocampal neurons (Diaz-Hernandez et al. 2008). Wortmannin, a PI3K inhibitor, antagonized ATP-induced  $[\text{Ca}^{2+}]_i$  increases in retinal Müller glia (Fig. 5e and h). This suggests a sustained basal PI3K/p38 MAPK activity, and that cytoskeletal elements are essential for ATP-induced  $\text{Ca}^{2+}$  internalization, possibly through mechanisms leading to pore formation and indiscriminately entrance of extracellular  $\text{Ca}^{2+}$  (Faria et al. 2010). In relation to ATP-induced macroscopic currents, inhibitors of PI3K, MAPK, CAMKII and PKC (Fig. 4) promoted a dose-

dependent reduction of ionic currents. Curiously, when compared to mammalian mouse 2BH4 cells and primary mice peritoneal macrophages (Faria et al. 2010), avian Müller cells ionic currents were also dependent on PI3K, MAPK and PKC (Fig. 4). However, cytoskeletal component inhibitors and connexin hemichannels (Fig. 3o) did not reduce ATP-induced macroscopic currents in avian Müller glia. This fact may be associated to interspecific differences between such cells in culture.

Our results also report that inhibition of PKC by Ro-8220, a bisindolylmaleimide (McKenna and Hanson 1993), CBX, a gap junction uncoupler (Li et al. 2001) or calmidazolium, a calmodulin-dependent phosphodiesterase and  $\text{Ca}^{2+}$ -transporting ATPase inhibitor (Gietzen 1983), significantly reduced calcium response to ATP (Fig. 5e, f, g and h). Interestingly, calmidazolium has been shown to cause elevation of  $[\text{Ca}^{2+}]_i$  in HeLa cells, but independently of calmodulin inhibition (Peppiatt et al. 2004). Also, it does not occur through store-operated  $\text{Ca}^{2+}$  entry mechanisms, as those activated by ATP (Peppiatt et al. 2004). In our hands, Müller cells exposed to calmidazolium showed no significant calcium transients in the presence of ATP.

In relation to the role of PKC, a calcium activated enzyme, reduction in ATP-induced calcium influx by the selective inhibitor Ro-8220 may be due to competitive inhibition of PKC, as seen with other bisindolylmaleimides, such as GF109203X (Beltman et al. 1996). Indeed, it was recently shown that Ro-31-8220 inhibits organic cation transporter 1 and other transporters activity (Mayati et al. 2015), which may further influence calcium influx by ATP in Müller cells. Among diverse large conductance pore antagonists tested against ATP-induced macroscopic currents, only Ruthenium red (RU-2), a general transient receptor potential (TRP) inhibitor reduced ATP effect in Müller cells (Fig. 3). The selective TRPV1 antagonist did not affect this event in contrast to mammalian Müller cells (Fig. 3n). Possibly other TRP members might have a role to constitute ATP induced channels such as TRPC 1 or 4 in the avian retina (Crousillac et al. 2003) TRPVs or TRPA1.

Müller cells are the main type of glia present in the retina, interacting with most, if not all neurons in this tissue. Data on the behavior of P2X family indicate that the activation of these receptors is involved in the modulation of neurotransmitter

**Table 1** Signalling associated to P2X7R mediated ionic currents,  $\text{Ca}^{2+}$  mobilization, and dye uptake

Measurements/ Proteins	CamK-II	PKC	Microtubule	PI-3 K	TRP	Connexin	MAPK
Ionic currents	++	+++	No	++	++	No	+++
Calcium mobilization	+	++	No	++	+	+++	+++
Dye uptake	No	+++	+++	++	No	No	+++

No inhibition (No). Inhibition inferior to 50% (+). Inhibition between 50 and 75% (++) . Inhibition superior to 75% (+++). Inhibition data were based on bar graph results

uptake (Ancasasi et al. 2013), DNA synthesis rate and proliferation of Müller glial cells, especially under pathologic conditions (Bringmann et al. 2001). Most of the transmitters found in the brain are also detected in the retinal tissue, and glial cells are active elements in the synthesis, release, signaling and uptake of major mediators of synaptic function (de Melo Reis et al. 2008). Retinal cells are assembled through chemical and electrical synapses, in particular glial cells, that express connexin 43 (Zahs and Ceelen 2006; Muto et al. 2014). Curiously, it has been reported that ATP is secreted from Müller glia in a connexin dependent manner (Bruckner et al. 2012). Therefore, our results support the role of gap junction uncouplers, such as CBX, that inhibits P2X7-associated pores. While fenamate is shown to act as a competitive antagonist, CBX is a non-competitive pore antagonist (Sudicani et al. 2006); thus, our data strongly corroborates with this proposition, once CBX had a significant impact on  $[Ca^{2+}]_i$  increase upon ATP stimulation. Calmidazolium, however, may act exclusively by blocking activation of ionic channel and transport of divalent cations, being unable to prevent the formation of the large permeabilizing pore (Virginio et al. 1997). Addition of calmidazolium significantly inhibited ATP-induced calcium transients (Fig. 5), but it had no effect on  $[Ca^{2+}]_i$  shifts as observed for CBX or SB203580. When compared to ionic currents, the unique difference was related to connexin hemichannel participation. Regarding to this, P2Y2R activation induced by ATP may increase  $[Ca^{2+}]_i$ , leading to membrane depolarization and consequently ATP release via connexin and/or pannexin-1 hemichannels (Zhang et al. 2012).

ATP induced dye uptake in avian Müller cells similarly to a previous report (Faria et al. 2016). MAPK, PI3K, PKC or cytoskeletal antagonists impaired ATP-induced dye uptake (Figs. 6 and 8). The same was observed in 2BH4 cells and peritoneal macrophages in terms of dye uptake inhibition in the presence of antagonists to these intracellular signaling pathways (Faria et al. 2010). In addition, cytoskeletal inhibitors did not affect macroscopic ionic currents or intracellular calcium, but inhibited dye uptake. This might suggest a type of conservation in the pore intracellular machinery that may be related to functions such as cytokine or transmitter release or cell death-mediated mechanisms. ATP-induced dye uptake was not modulated by CAMKII, TRP channels or connexins, as observed for ionic currents and intracellular calcium mobilization (Table 1).

Finally, avian Müller glia release ATP through a calcium-dependent exocytotic mechanism by glutamate (Loiola and Ventura 2011) while rat retinal slices released ATP by vesicle independent mechanisms induced by glutamate (Voigt et al. 2015). Activation of P2X7R evokes cell death of developing retinal neurons at early periods of retinal differentiation in a glutamate-independent (but P2X7R-dependent) manner in mixed co-cultured neurons and glial cells (Ancasasi et al.

2013). Recently, we showed that purified Müller cells are selectively activated by GSH (Freitas et al. 2016). GSH induces calcium shifts in Müller cells and secretes GABA in mixed neuron-glia or in purified Müller cell cultures. These effects are mediated by P2X7R and could have a major effect on neuroprotection of retinal cells.

In conclusion, we extended knowledge on the modulation of P2X7R using avian Müller glia cells in culture. We showed that large conductance channels are not involved in the ATP-induced dye uptake, but signaling intermediates such as MAPK, PI3K, or PK are intrinsically associated to pore formation mechanisms. Discovery of intracellular purinergic regulation sites in the radial (Müller) glia may present novel targets for therapeutic interventions in retinal diseases, such as age-related macular degeneration and developmental impairments.

BBG, brilliant blue G; BSA, bovine serum albumin; BzATP, benzoyl-benzoyl ATP; CAMKII,  $Ca^{2+}$ -calmodulin kinase II; CBX, carbenoxolone; MAPK, mitogen activated protein kinase; oATP, oxidized ATP; P2X7R, P2X7receptor; Panx-1, pannexin-1; PBS, phosphate-buffered saline; PI, propidium iodide; PI3-K, phosphoinositide 3-kinase; PKC, protein kinase C; RU-2, Ruthenium red; TRP, transient receptor potential.

**Acknowledgements** We are indebted to the technical support of Luciano C. Ferreira.

**Authors' contributions** Robson Faria performed the experiments, analyzed and interpreted data, prepared figures and wrote the paper. Ricardo Reis prepared Müller glia cells in culture and wrote the paper. Hércules Freitas prepared Müller glia cells in culture, performed single cell calcium imaging assays, analyzed data and wrote the paper. All authors read and approved the final manuscript.

#### Compliance with ethical standards

**Ethics approval and consent to participate** All experiments involving animals were approved by and carried out in accordance with the guidelines of the Animal Care and Use Committee of the Biophysics Institute (CEUA permit number IBCCF-035). Efforts were made to minimize animal suffering.

**Consent for publication** Not applicable.

**Availability of data and materials** The datasets used and/or analyzed during the current study available from the corresponding author on reasonable request.

**Competing interests** The authors state that they have no competing financial interests.

**Funding** This work was supported by Conselho Nacional de Desenvolvimento Científico e Tecnológico (CNPq), Fundação de Amparo à Pesquisa do Estado do Rio de Janeiro (FAPERJ), Oswaldo Cruz Institute, and Instituto Nacional de Ciência e Tecnologia de Neurociência Translacional (INCT-INNT). Hércules R. Freitas is recipient of a CNPq Ph.D. fellowship; RAMR has a research fellowship (CNPq).

## References

- Ancas RM, Ornelas IM, Cossenza M, Persechini PM, Ventura AL (2013) ATP induces the death of developing avian retinal neurons in culture via activation of P2X7 and glutamate receptors. Purinergic signalling 9(1):15–29. doi:10.1007/s11302-012-9324-5
- Barros-Barbosa AR, Lobo MG, Ferreirinha F, Correia-de-Sa P, Cordeiro JM (2015) P2X7 receptor activation downmodulates Na(+)-dependent high-affinity GABA and glutamate transport into rat brain cortex synaptosomes. Neuroscience 306:74–90. doi:10.1016/j.neuroscience.2015.08.026
- Bartlett R, Stokes L, Sluyter R (2014) The P2X7 receptor channel: recent developments and the use of P2X7 antagonists in models of disease. Pharmacol Rev 66(3):638–675. doi:10.1124/pr.113.008003
- Beltman J, McCormick F, Cook SJ (1996) The selective protein kinase C inhibitor, Ro-31-8220, inhibits mitogen-activated protein kinase phosphatase-1 (MKP-1) expression, induces c-Jun expression, and activates Jun N-terminal kinase. J Biol Chem 271(43):27018–27024
- Bringmann A, Pannicke T, Moll V, Milenkovic I, Faude F, Enzmann V, Wolf S, Reichenbach A (2001) Upregulation of P2X(7) receptor currents in Muller glial cells during proliferative vitreoretinopathy. Invest Ophthalmol Vis Sci 42(3):860–867
- Bruckner E, Grosche A, Pannicke T, Wiedemann P, Reichenbach A, Bringmann A (2012) Mechanisms of VEGF- and glutamate-induced inhibition of osmotic swelling of murine retinal glial (Muller) cells: indications for the involvement of vesicular glutamate release and connexin-mediated ATP release. Neurochem Res 37(2):268–278. doi:10.1007/s11064-011-0606-z
- Burnstock G (2015) Physiopathological roles of P2X receptors in the central nervous system. Curr Med Chem 22(7):819–844
- Butt AM (2011) ATP: a ubiquitous gliotransmitter integrating neuronal-glia networks. Semin Cell Dev Biol 22(2):205–213. doi:10.1016/j.semcdb.2011.02.023
- Crousillac S, LeRouge M, Rankin M, Gleason E (2003) Immunolocalization of TRPC channel subunits 1 and 4 in the chicken retina. Vis Neurosci 20(4):453–463
- De Melo Reis RA, Schitine CS, Kofalvi A, Grade S, Cortes L, Gardino PF, Malva JO, de Mello FG (2011) Functional identification of cell phenotypes differentiating from mice retinal neurospheres using single cell calcium imaging. Cell Mol Neurobiol 31(6):835–846. doi:10.1007/s10571-011-9673-6
- Diaz-Hernandez M, del Puerto A, Diaz-Hernandez JI, Diez-Zaera M, Lucas JJ, Garrido JJ, Miras-Portugal MT (2008) Inhibition of the ATP-gated P2X7 receptor promotes axonal growth and branching in cultured hippocampal neurons. J Cell Sci 121(Pt 22):3717–3728. doi:10.1242/jcs.034082
- Donnelly-Roberts DL, Namovic MT, Han P, Jarvis MF (2009) Mammalian P2X7 receptor pharmacology: comparison of recombinant mouse, rat and human P2X7 receptors. Br J Pharmacol 157(7):1203–1214. doi:10.1111/j.1476-5381.2009.00233.x
- Eastlake K, Banerjee PJ, Angbohng A, Charteris DG, Khaw PT, Limb GA (2016) Muller glia as an important source of cytokines and inflammatory factors present in the gliotic retina during proliferative vitreoretinopathy. Glia 64(4):495–506. doi:10.1002/glia.22942
- Faria RX, Defarias FP, Alves LA (2005) Are second messengers crucial for opening the pore associated with P2X7 receptor? Am J Phys Cell Physiol 288(2):C260–C271. doi:10.1152/ajpcell.00215.2004
- Faria RX, Reis RA, Casabulho CM, Alberto AV, de Farias FP, Henriques-Pons A, Alves LA (2009) Pharmacological properties of a pore induced by raising intracellular Ca2+. Am J Phys Cell Physiol 297(1):C28–C42. doi:10.1152/ajpcell.00476.2008
- Faria RX, Casabulho CM, Reis RA, Alves LA (2010) Large-conductance channel formation mediated by P2X7 receptor activation is regulated through distinct intracellular signaling pathways in peritoneal macrophages and 2BH4 cells. Naunyn Schmiedeberg's Arch Pharmacol 382(1):73–87. doi:10.1007/s00210-010-0523-8
- Faria RX, Reis RA, Ferreira LG, Cezar-de-Mello PF, Moraes MO (2016) P2X7R large pore is partially blocked by pore forming proteins antagonists in astrocytes. J Bioenerg Biomembr 48(3):309–324. doi:10.1007/s10863-016-9649-9
- Freitas HR, Ferraz G, Ferreira GC, Ribeiro-Resende VT, Chiarini LB, do Nascimento JL, Matos Oliveira KR, Pereira TL, Ferreira LG, Kubrusly RC, Faria RX, Herculano AM, Reis RA (2016) Glutathione-induced calcium shifts in Chick retinal glial cells. PLoS One 11(4):e0153677. doi:10.1371/journal.pone.0153677
- Gietzen K (1983) Comparison of the calmodulin antagonists compound 48/80 and calmidazolium. Biochem J 216(3):611–616
- Hamburger V, Hamilton HL (1951) A series of normal stages in the development of the chick embryo. J Morphol 88(1):49–92
- Jacobson KA, Muller CE (2016) Medicinal chemistry of adenosine, P2Y and P2X receptors. Neuropharmacology 104:31–49. doi:10.1016/j.neuropharm.2015.12.001
- Li J, Shen H, Naus CC, Zhang L, Carlen PL (2001) Upregulation of gap junction connexin 32 with epileptiform activity in the isolated mouse hippocampus. Neuroscience 105(3):589–598
- Loiola EC, Ventura AL (2011) Release of ATP from avian Muller glia cells in culture. Neurochem Int 58(3):414–422. doi:10.1016/j.neuint.2010.12.019
- Magni G, Ceruti S (2014) The purinergic system and glial cells: emerging costars in nociception. Biomed Res Int 2014:495789. doi:10.1155/2014/495789
- Mayati A, Bruyere A, Moreau A, Jouan E, Denizot C, Parmentier Y, Fardel O (2015) Protein kinase C-independent inhibition of organic cation transporter 1 activity by the bisindolylmaleimide Ro 31-8220. PLoS One 10(12):e0144667. doi:10.1371/journal.pone.0144667
- McKenna JP, Hanson PJ (1993) Inhibition by Ro 31-8220 of acid secretory activity induced by carbachol indicates a stimulatory role for protein kinase C in the action of muscarinic agonists on isolated rat parietal cells. Biochem Pharmacol 46(4):583–588
- de Melo Reis RA, Ventura AL, Schitine CS, de Mello MC, de Mello FG (2008) Muller glia as an active compartment modulating nervous activity in the vertebrate retina: neurotransmitters and trophic factors. Neurochem Res 33(8):1466–1474. doi:10.1007/s11064-008-9604-1
- Muto T, Tien T, Kim D, Sarthy VP, Roy S (2014) High glucose alters Cx43 expression and gap junction intercellular communication in retinal Muller cells: promotes Muller cell and pericyte apoptosis. Invest Ophthalmol Vis Sci 55(7):4327–4337. doi:10.1167/iovs.14-14606
- Newman EA (2015) Glial cell regulation of neuronal activity and blood flow in the retina by release of gliotransmitters. Philos Trans R Soc Lond Ser B Biol Sci 370(1672). doi:10.1098/rstb.2014.0195
- Niyadurupola N, Sidaway P, Ma N, Rhodes JD, Broadway DC, Sanderson J (2013) P2X7 receptor activation mediates retinal ganglion cell death in a human retina model of ischemic neurodegeneration. Invest Ophthalmol Vis Sci 54(3):2163–2170. doi:10.1167/iovs.12-10968
- Pannicke T, Fischer W, Biedermann B, Schadlich H, Grosche J, Faude F, Wiedemann P, Allgaier C, Illes P, Burnstock G, Reichenbach A (2000) P2X7 receptors in Muller glial cells from the human retina. J Neurosci 20(16):5965–5972
- Peppiatt CM, Holmes AM, Seo JT, Bootman MD, Collins TJ, McDonald F, Roderick HL (2004) Calmidazolium and arachidonate activate a calcium entry pathway that is distinct from store-operated calcium influx in HeLa cells. Biochem J 381(Pt 3):929–939. doi:10.1042/bj20040097
- Reichenbach A, Bringmann A (2016) Purinergic signaling in retinal degeneration and regeneration. Neuropharmacology 104:194–211. doi:10.1016/j.neuropharm.2015.05.005

- Reis R, da Silva M, dos Santos N, Bampton E, Taylor J, de Mello F, Linden R (2002) Sympathetic neuronal survival induced by retinal trophic factors. *J Neurobiol* 50(1):13–23. doi:[10.1002/neu.10008](https://doi.org/10.1002/neu.10008)
- Sanches G, de Alencar LS, Ventura AL (2002) ATP induces proliferation of retinal cells in culture via activation of PKC and extracellular signal-regulated kinase cascade. *Int J Dev Neurosci* 20(1):21–27
- Schitine CS, Mendez-Flores OG, Santos LE, Ornelas I, Calaza KC, Perez-Toledo K, Lopez-Bayghen E, Ortega A, Gardino PF, de Mello FG, Reis RA (2015) Functional plasticity of GAT-3 in avian Muller cells is regulated by neurons via a glutamatergic input. *Neurochem Int* 82:42–51. doi:[10.1016/j.neuint.2015.02.004](https://doi.org/10.1016/j.neuint.2015.02.004)
- Skaper SD (2011) Ion channels on microglia: therapeutic targets for neuroprotection. *CNS Neurol Disord Drug Targets* 10(1):44–56
- Suadicani SO, Brosnan CF, Scemes E (2006) P2X7 receptors mediate ATP release and amplification of astrocytic intercellular Ca<sup>2+</sup> signaling. *J Neurosci* 26(5):1378–1385. doi:[10.1523/jneurosci.3902-05.2006](https://doi.org/10.1523/jneurosci.3902-05.2006)
- Tewari M, Seth P (2015) Emerging role of P2X7 receptors in CNS health and disease. *Ageing Res Rev* 24(Pt B):328–342. doi:[10.1016/j.arr.2015.10.001](https://doi.org/10.1016/j.arr.2015.10.001)
- Tong L, Beuerman R, Simonyi S, Hollander DA, Stern ME (2016) Effects of Punctal occlusion on clinical signs and symptoms and on tear cytokine levels in patients with dry eye. *Ocul Surf* 14(2):233–241. doi:[10.1016/j.jtos.2015.12.004](https://doi.org/10.1016/j.jtos.2015.12.004)
- Verderio C, Matteoli M (2011) ATP in neuron-glia bidirectional signaling. *Brain Res Rev* 66(1–2):106–114. doi:[10.1016/j.brainresrev.2010.04.007](https://doi.org/10.1016/j.brainresrev.2010.04.007)
- Verkhatsky A, Steinhauser C (2000) Ion channels in glial cells. *Brain Res Brain Res Rev* 32(2–3):380–412
- Virginio C, Church D, North RA, Surprenant A (1997) Effects of divalent cations, protons and calmidazolium at the rat P2X7 receptor. *Neuropharmacology* 36(9):1285–1294
- Voigt J, Grosche A, Vogler S, Pannicke T, Hollborn M, Kohen L, Wiedemann P, Reichenbach A, Bringmann A (2015) Nonvesicular release of ATP from rat retinal glial (Muller) cells is differentially mediated in response to osmotic stress and glutamate. *Neurochem Res* 40(4):651–660. doi:[10.1007/s11064-014-1511-z](https://doi.org/10.1007/s11064-014-1511-z)
- Volonte C, Apolloni S, Skaper SD, Burnstock G (2012) P2X7 receptors: channels, pores and more. *CNS Neurol Disord Drug Targets* 11(6):705–721
- Yan Z, Khadra A, Li S, Tomic M, Sherman A, Stojilkovic SS (2010) Experimental characterization and mathematical modeling of P2X7 receptor channel gating. *J Neurosci* 30(42):14213–14224. doi:[10.1523/jneurosci.2390-10.2010](https://doi.org/10.1523/jneurosci.2390-10.2010)
- Zahs KR, Ceelen PW (2006) Gap junctional coupling and connexin immunoreactivity in rabbit retinal glia. *Vis Neurosci* 23(1):1–10. doi:[10.1017/s0952523806231018](https://doi.org/10.1017/s0952523806231018)
- Zhang M, Piskuric NA, Vollmer C, Nurse CA (2012) P2Y2 receptor activation opens pannexin-1 channels in rat carotid body type II cells: potential role in amplifying the neurotransmitter ATP. *J Physiol* 590(17):4335–4350. doi:[10.1113/jphysiol.2012.236265](https://doi.org/10.1113/jphysiol.2012.236265)
- Zou L, Tu G, Xie W, Wen S, Xie Q, Liu S, Li G, Gao Y, Xu H, Wang S, Xue Y, Wu B, Lv Q, Ying M, Zhang X, Liang S (2016) LncRNA NONRATT021972 involved the pathophysiologic processes mediated by P2X7 receptors in stellate ganglia after myocardial ischemic injury. *Purinergic signalling* 12(1):127–137. doi:[10.1007/s11302-015-9486-z](https://doi.org/10.1007/s11302-015-9486-z)